Passivity Test of Immittance Descriptor Systems Based on Generalized Hamiltonian Methods

Zheng Zhang, *Student Member, IEEE* and Ngai Wong, *Member, IEEE*

***Abstract*—A generalized Hamiltonian method (GHM) and its half-size variant (HGHM) are proposed to characterize the spectral behaviors of descriptor systems (DSs). With the preprocess ImPT (Improper Part Test), GHM and HGHM can be applied to test the passivity of immittance (impedance or admittance) DSs without system decomposition, system index assumption or minimal realization requirement, which are the major bottlenecks of existing algebraic DS passivity tests. The proposed method allows exact detection of nonpassive frequency intervals which is not possible with frequency sweeping techniques. Numerical results confirm the effectiveness of the proposed methods.**

***Index Terms*—Descriptor system, GHM, HGHM, passivity.**

I. Introduction

THIS work is motivated by the demand of passive modeling of on-chip components and electrical circuits in VLSI simulations [1]–[3]. Passivity can be interpreted as the inability of a system to generate energy internally, which is of great importance for stable global simulations. However, nonpassive models may be generated from some stability-preserving algorithms (e.g., vector fitting (VF) [4] and Páde approximation via Lanczos algorithm [1]) or even some theoretically passivity-preserving techniques (e.g., [2]) on finite-precision machines. As a remedy, passivity enforcement techniques [3] can eliminate or mitigate passivity violations. These enforcements need to locate the possible nonpasive regions via passivity test in advance. For regular (or nonsingular) systems, numerous passivity assessments have been proposed. The reader is referred to [3], [5] and the references therein.

As a superset of regular state-space system, descriptor systems (DSs) [6], [7] are widely used in VLSI simulations [2], [8]. Nevertheless, DS passivity tests are much less developed compared with their regular system counterparts. The $O(n^6)$ computation renders the extended LMI (linear matrix inequation) tests [9], [10] impractical for general DSs. Ref. [10] presented a cheaper method based on generalized Schur decomposition, but it posed strict restrictions on system observability and controllability. Some literatures assess positive realness via generalized algebraic Riccati equations (GAREs) [11], [12], but the admissible requirement is also very strong for practical physical models. Furthermore, none of these methods can locate the nonpassive frequency regions, which is normally required in testing the validity of circuit and component models. Some decompose-and-test flows [13], [14] require the DSs to be minimal, and the system decomposition and transformation may induce large numerical errors (caused by possibly ill-conditioned matrix inversions). The eigenvalue-based DS passivity test in [15] is only applicable to scalar functions. Frequency sweeping methods [16], [17] detect nonpassive regions at a set of frequency points, but they may miss nonpassive frequency intervals. Therefore, it is desirable to develop a passivity assessment that can identify the nonpassive regions of general DSs efficiently and accurately.

We propose, for the first time, a flexible passivity test for general DSs based on generalized Hamiltonian methods. The main contribution of this paper includes: 1) GHM and HGHM, to characterize the eigenvalues of DS spectral functions; 2) A complete DS passivity test based on ImPT, GHM and HGHM to test the improper and proper parts easily without system decomposition; 3) The observation that the GHM- and HGHM-based passivity tests are the supersets of traditional Hamiltonian method and its half-size [5] counterpart, respectively, as well as the connection of GHM with GAREs [11], [12]. A preliminary version of this work, which does not contain HGHM and related results, was presented in [18].

II. Preliminaries of LTI System Passivity

For an immittance linear time-invariant (LTI) system, the (strict) passivity is equivalent to its square transfer matrix $H(s)$ being (strictly) positive real [9]:

1) $\underline{H(s)}$ has no poles in $\mathbf{Re}[s] > 0$;
2) $\overline{H(s)} = H(\bar{s})$ where $\bar{o}$ stands for the conjugate of o;
3) The spectral function $G(j\omega) = \frac{H(j\omega)+H^*(j\omega)}{2} \geq 0$ for all $\omega \in \mathbb{R}$ ($>$ for strict positive realness), where * means the conjugate transpose operation.

For a regular state-space system $H(s) = C(sI-A)^{-1}B + D$, its passivity can be tested by the Hamiltonian matrix [5]:

$$M = \begin{bmatrix} \hat{A} & -\hat{R} \\ \hat{P} & -\hat{A}^T \end{bmatrix} \tag{1}$$

of which any purely imaginary eigenvalue defines a boundary frequency of passivity violations. In (1), $\hat{A} = A - B(D + D^T)^{-1}C$, $\hat{R} = B(D+D^T)^{-1}B^T$ and $\hat{P} = C^T(D+D^T)^{-1}C$.

In circuit or system simulations, we usually use the LTI DS:

$$E\dot{x} = Ax + Bu, \quad y = Cx + Du, \tag{2}$$

where $x \in \mathbb{R}^n$ denotes the state variables, $E, A \in \mathbb{R}^{n\times n}$, $B, C^T \in \mathbb{R}^{n\times m}$, $D \in \mathbb{R}^{m\times m}$, and $rank(E) \leq n$ ("="

The authors are with the Department of Electrical and Electronic Engineering, The University of Hong Kong, Pokfulam Road, Hong Kong (e-mail: {zzhang, nwong}@eee.hku.hk). This work was supported in part by Hong Kong Research Grants Council under Project HKU 717407E, the University Research Committee of The University of Hong Kong.

Copyright (c) 2009 IEEE. Personal use of this material is permitted. However, permission to use this material for any other purposes must be obtained from the IEEE by sending an email to pubs-permissions@ieee.org.

corresponds to regular cases). The transfer matrix of (2) is

$$H(s) = C(sE - A)^{-1}B + D. \quad (3)$$

Here (A, E) is assumed to be regular, i.e., $det(sE - A)$ is not identically zero. There exists a Weierstrass form [9]:

$$(A, E) = W(\begin{bmatrix} F & 0 \\ 0 & I_{n-q} \end{bmatrix}, \begin{bmatrix} I_q & 0 \\ 0 & N \end{bmatrix})T, \quad (4)$$

where W and T are nonsingular, I_q denotes an identity matrix of dimension q, F and N (an index-μ nilpotent matrix, i.e., $N^\mu = 0$ and $N^{\mu-1} \neq 0$) correspond to the finite and infinite generalized eigenvalues of (A, E), respectively. The Weierstrass form tells

$$H(s) = \underbrace{C_p(sI_q - F)^{-1}B_p + M_0}_{H_p(s)} + \underbrace{\sum_{k=1}^{\mu-1} s^k M_k}_{H_{imp}(s)}, \quad (5)$$

where $\begin{bmatrix} C_p & C_\infty \end{bmatrix} = CT^{-1}$ and $\begin{bmatrix} B_p \\ B_\infty \end{bmatrix} = W^{-1}B$, $M_0 = D - C_\infty B_\infty$, $M_k = -C_\infty N^k B_\infty$ $(k = 1, ..., \mu - 1)$. $H_p(s)$ and $H_{imp}(s)$ are the proper and improper parts, respectively.

The immittance DS in (5) is passive if and only if [9]: $H_p(s)$ is passive; $M_1 \geq 0$ and $M_k = 0$ for any $k \geq 2$.

III. GHM and HGHM Theories for DSs

A. GHM for General DSs

Theorem 1: Assume λ is not an eigenvalue of $\frac{D+D^T}{2}$ for the stable DS (E, A, B, C, D) (i.e., any finite s satisfying $det(A - sE) = 0$ is located on the left half plane), then λ is an eigenvalue of $G(j\omega)$ if and only if $j\omega$ is a generalized eigenvalue of the matrix pencil $(J,\ K)$ defined as

$$(J, K) = (\begin{bmatrix} A + BQ^{-1}C & BQ^{-1}B^T \\ -C^TQ^{-1}C & -A^T - C^TQ^{-1}B^T \end{bmatrix}, \begin{bmatrix} E & 0 \\ 0 & E^T \end{bmatrix}), \quad (6)$$

where $Q = (2\lambda I - D - D^T)$.

Proof: Assume λ is an eigenvalue of the spectral function $G(j\omega)$. Since $H^*(j\omega) = H^T(-j\omega)$, we have $x \neq 0$ such that

$$2G(j\omega)x = \{\begin{bmatrix} C & B^T \end{bmatrix} \Omega_\omega^{-1} \begin{bmatrix} B \\ -C^T \end{bmatrix} + D + D^T\}x = 2\lambda x. \quad (7)$$

Here $\Omega_\omega = \begin{bmatrix} j\omega E - A & \\ & j\omega E^T + A^T \end{bmatrix}$. We rewrite (7) as

$$Q^{-1} \begin{bmatrix} C & B^T \end{bmatrix} z = x \quad (8)$$

with $z = \Omega_\omega^{-1} \begin{bmatrix} B \\ -C^T \end{bmatrix} x \neq 0$. Equation (8) implies

$$\Omega_\omega^{-1} \begin{bmatrix} B \\ -C^T \end{bmatrix} Q^{-1} \begin{bmatrix} C & B^T \end{bmatrix} z = z, \quad (9)$$

which is equivalent to

$$Jz = j\omega K z. \quad (10)$$

Conversely, denoting $w := Q^{-1} \begin{bmatrix} C & B^T \end{bmatrix} z$ ($w \neq 0$, observed in (9)) and pre-multiplying both sides of (9) by $Q^{-1} \begin{bmatrix} C & B^T \end{bmatrix}$, we reach

$$Q^{-1} \begin{bmatrix} C & B^T \end{bmatrix} \Omega_\omega^{-1} \begin{bmatrix} B \\ -C^T \end{bmatrix} w = w, \quad (11)$$

which is equivalent to (7), implying λ is an eigenvalue of $G(j\omega)$. ■

B. HGHM for Symmetric DSs

Theorem 2: For symmetric DSs, if λ is not an eigenvalue of D, (J, K) defined in (6) reduces to a half-size matrix pencil

$$(J_h, K_h) = (A + B(\lambda I - D)^{-1}C,\ EA^{-1}E), \quad (12)$$

and the generalized eigenvalue $j\omega$ is replaced by $\beta = \omega^2$.

Proof: For symmetric DS, $H^*(j\omega) = H(-j\omega) = -C(j\omega E + A)^{-1}B + D$, and (J, K) can be written as

$$(J, K) = (\begin{bmatrix} S & T \\ -T & -S \end{bmatrix}, \begin{bmatrix} E & 0 \\ 0 & E \end{bmatrix}), \quad (13)$$

where $S = A + B(2\lambda I - 2D)^{-1}C, T = B(2\lambda I - 2D)^{-1}C$. Noting $(J', K') = Z(J, K)Z^T$ has the same generalized eigenvalues with (J, K) if Z is invertible, we set $Z = \begin{bmatrix} I & I \\ I & -I \end{bmatrix}$ and get

$$(J', K') = (\begin{bmatrix} 0 & 2(S - T) \\ 2(S + T) & 0 \end{bmatrix}, \begin{bmatrix} 2E & \\ & 2E \end{bmatrix}). \quad (14)$$

Assume λ is an eigenvalue of $G(j\omega)$, then $j\omega$ is also a generalized eigenvalue of (J', K'), and there exists

$$\begin{bmatrix} -j\omega E & S - T \\ S + T & -j\omega E \end{bmatrix} \begin{bmatrix} x_1 \\ x_2 \end{bmatrix} = 0, \quad \begin{bmatrix} x_1 \\ x_2 \end{bmatrix} \neq 0, \quad (15)$$

which can be further reduced to

$$(J_h - \omega^2 K_h)x_1 = 0,\ \ x_1 \neq 0. \quad (16)$$

Therefore, $\beta = \omega^2$ is a generalized eigenvalue of (J_h, K_h).

Conversely, setting $x_2 = j\omega(S - T)^{-1}x_1$, we can arrive at (15) from (16) and then Theorem 1. ■

IV. DS Passivity Test

A. Testing the Improper Part by ImPT

Denoting the highest order of $H_{imp}(s)$ by the integer $\zeta - 1$ $(1 \leq \zeta \leq \mu)$, we propose **ImPT** to characterize the improper part of a DS. Given a set of positive real scalars s_i $(i = 1, 2, ...)$ with $s_{i+1} = \eta s_i$ $(\eta > 1)$, the matrix norm of $H(s_i)$ is

$$\|H(s_i)\| = s_i^{\zeta-1} \left\| M_{\zeta-1} + \frac{M_{\zeta-2}}{s_i} + \cdots + \frac{H_p(s_i)}{s_i^{\zeta-1}} \right\|. \quad (17)$$

If s_i is large enough, $s_i^{\zeta-1}M_{\zeta-1}$ dominates $H(s_i)$. In this case, we have $M_{\zeta-1} + \frac{M_{\zeta-2}}{s_i} + \cdots + \frac{H_p(s_i)}{s_i^{\zeta-1}} \approx M_{\zeta-1}$ and

$$\frac{\|H(s_{i+1})\|}{\|H(s_i)\|} \approx \eta^{\zeta-1}. \quad (18)$$

Therefore, the system index can be computed by

$$\zeta = \left[\log_\eta(\frac{\|H(s_{i+1})\|}{\|H(s_i)\|})\right] + 1, \quad (19)$$

where $[o]$ represents rounding. In practical implementations, η can be set around $10 - 100$, and we may start with a randomly selected number (e.g., $s_1 = 10^5$) and then replace s_i with s_{i+1} until $\left| \left[\log_\eta(\frac{\|H(s_{i+1})\|}{\|H(s_i)\|})\right] - \log_\eta(\frac{\|H(s_{i+1})\|}{\|H(s_i)\|}) \right| < \delta$. Here δ is a small positive constant used to control numerical errors. Since s_i is exponentially increased, the iteration can converge very

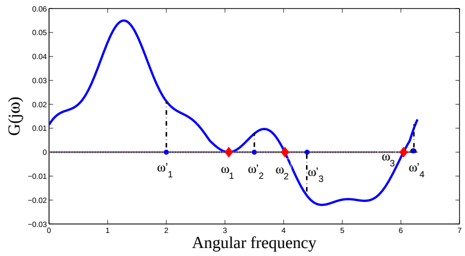

Fig. 1. An illustrative example for nonpassive region identification.

fast. If $\zeta \geq 3$, we have $M_2 \neq 0$ and the DS is nonpassive. In case $\zeta = 2$, $H(s_i) = H_p(s_i) + H_{imp}(s_i) \approx s_i M_1 + M_0$, then

$$M_1 \approx \frac{H(s_{i+1}) - H(s_i)}{s_{i+1} - s_i}. \quad (20)$$

With a numerical error control, (20) can also be used to compute M_1 with a high accuracy. In impulse-free DSs, the denominator in (19) might approach zero in case $M_0 = 0$, so (19) may give erroneous results. In this case, we replace $H(s_i)$ with $H(s_i) + I_m$ to compute ζ.

Hereafter, we assume that $H_{imp}(s)$ has been checked by ImPT, $\zeta \leq 2$, and $M_1 \geq 0$ (or else the passivity test terminates since we have already known the improper part is nonpassive). In this case $H_p(j\omega) + H_p^*(j\omega) = H(j\omega) + H^*(j\omega)$.

B. Testing the Proper Part by GHM and HGHM

Setting $\lambda = 0$, we have $(J, K) = (J_0, K_0)$ with

$$J_0 = M = \begin{bmatrix} \hat{A} & -\hat{R} \\ \hat{P} & -\hat{A} \end{bmatrix}, \quad K_0 = K. \quad (21)$$

Here M is the Hamiltonian matrix defined in (1). We note that this matrix pencil is used in [19], but it is just a special case of GHM. Besides passivity assessment, the proposed GHM theory may have potential use in the passivity enforcement of descriptor-form models, which is under investigation. For HGHM, setting $\lambda = 0$ gives a half-size matrix pencil

$$(J_{h0}, K_{h0}) = (A - BD^{-1}C, \quad EA^{-1}E). \quad (22)$$

Any purely imaginary (or positive real) generalized eigenvalue $j\omega$ (or $\beta = \omega^2$) of (J_0, K_0) (or (J_{h0}, K_{h0}) for symmetric DSs) defines a crossover angular frequency ω. Assume $\Theta = \{\omega_1, ..., \omega_p\}$ where ω_i $(i = 1, ..., p)$ denotes the p crossover points obtained from GHM or HGHM, then the passive and nonpassive regions of $H(j\omega)$ can be identified as follows:

1. If Θ is empty, test $G(j\omega_0)$ at a randomly selected sampling point ω_0. The system is strictly passive if $G(j\omega_0) > 0$, otherwise nonpassive at any frequency point.
2. If Θ is not empty, test $G(j\omega_k')$ at $\omega_k' \in \ell_k$ $(k = 1, 2, ..., p{+}1)$ where $\ell_1 = (0, \omega_1)$, $\ell_i = (\omega_{i-1}, \omega_i)$ for $i = 2, ..., p$ and $\ell_{p+1} = (\omega_p, \infty)$. If $G(j\omega_k') > 0$, then the DS is passive in the interval ℓ_k, otherwise nonpassive in ℓ_k.

An illustrative example is shown in Fig. 1. For this DS, GHM and HGHM produce 3 crossover points. We randomly select one sampling point in each interval. Since $G(j\omega_3') < 0$ and $G(j\omega_k') > 0$ for $k = 1, 2, 4$, the DS is nonpassive in (ω_2, ω_3) but passive in other frequency bands.

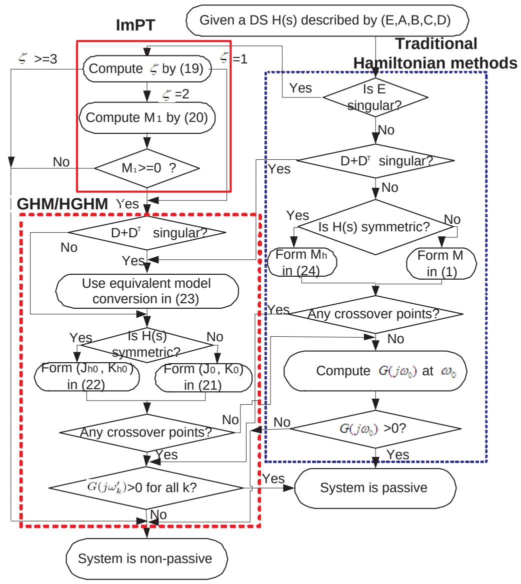

Fig. 2. The complete passivity test flow for DSs, including regular systems.

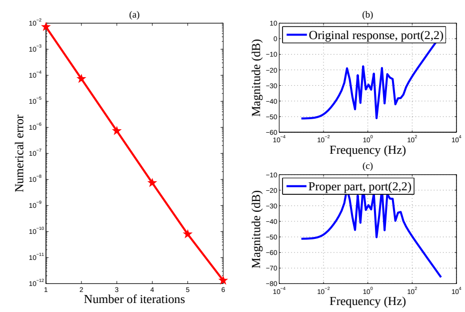

Fig. 3. ImPT test for the MNA model (the iteration # means i in (19)).

C. Equivalent Model Conversion

At the first glance, GHM/HGHM test requires $D + D^T$ to be nonsingular, which is not always satisfied in practical DSs. In this case, we need to perform an equivalent model conversion in advance. Assume that $\alpha \in \mathbb{R}$ is not an eigenvalue of D, then $D_\alpha = \alpha I - D$ is nonsingular. A new DS $H'(s)$ realized by (E', A', B', C', D') can be constructed as

$$E' = \begin{bmatrix} E & \\ & 0 \end{bmatrix}, \quad A' = \begin{bmatrix} A & \\ & D_\alpha^{-1} \end{bmatrix}, \quad B' = \begin{bmatrix} B \\ I \end{bmatrix}, \quad C' = \begin{bmatrix} C & I \end{bmatrix}, \quad D' = \alpha I. \quad (23)$$

We note $H'(s) = H(s)$, but $D' + D'^T$ and D' are nonsingular. Therefore, the proper part of $H(s)$ can be assessed by testing the passivity of $H'(s)$ via GHM or HGHM. The main computation in GHM and HGHM tests is the $O(n^3)$ generalized eigenvalue solution. HGHM-based test should be $8\times$ faster than GHM-based method due to its half-size nature.

D. Connection to the Traditional Hamiltonian Method and Half-size Singularity Test

For standard state-space models ($E = I$), the generalized eigenvalue solution of (J, K) reduces to the eigenvalue solution of J defined in (6), which has been widely used in

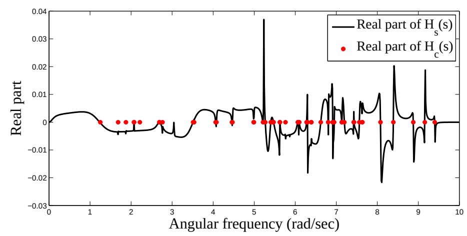

Fig. 4. GHM and frequency sweeping results for the PEEC model.

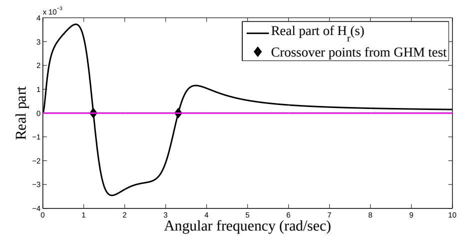

Fig. 5. Real part of $H_r(s)$.

passivity enforcements [3]. To check passivity, we set $\lambda = 0$ and get $J_0 = M$ (defined in (1)). For symmetric regular systems, the generalized eigenvalue solution of (J_{h0}, K_{h0}) in (22) can be replaced by the eigenvalue solution of

$$M_h = A(A - BD^{-1}C), \qquad (24)$$

which is the half-size singularity test firstly proposed in [5].

Therefore, Hamiltonian method and its half-size variant are special cases of GHM and HGHM, respectively. All of them detect passivity violation regions by finding boundary frequencies, but GHM and HGHM can deal with DSs as well as regular systems without restrictions on D. The complete test flow is illustrated in Fig. 2.

E. Strict Positive Realness of Impulse-free DSs

GARE [11], [12] is widely used to characterize the positive realness of impulse-free DSs. This part shows its connection with GHM. Suppose (A, E) is regular, impulse-free and $D + D^T > 0$, then the following statements are equivalent.

1) $H(s)$ is strictly positive real.

2) The generalized algebraic Riccati equation (GARE)

$$\hat{A}^T X + X^T \hat{A} + X^T \hat{R} X + \hat{P} = 0,\ E^T X = X^T E \geq 0 \qquad (25)$$

has a solution X such that $(\hat{A} + \hat{R}X, E)$ is stable.

3) The matrix pencil (J_0, K_0) has no purely imaginary generalized eigenvalues and $M_0 > 0$ (M_0 is defined in (5)).

Proof: The equivalence of 1) and 2) has been proved in [11]. 3)⇒1) is obvious. From Statement 2), we get

$$\begin{aligned} &\det(J_0 - sK_0) = \det(\begin{bmatrix} I & \\ -X^T & I \end{bmatrix} (J_0 - sK_0) \begin{bmatrix} I & \\ X & I \end{bmatrix}) \\ &= \det(\begin{bmatrix} sE - (\hat{A} + \hat{R}X) & 0 \\ 0 & sE^T + (\hat{A}^T + X^T\hat{R}^T) \end{bmatrix}) \\ &= \det(sE - (\hat{A} + \hat{R}X)) \det(sE + (\hat{A} + \hat{R}X)). \end{aligned} \qquad (26)$$

Since $(\hat{A} + \hat{R}X, E)$ is stable, $\hat{A} + \hat{R}X \pm j\omega E$ is nonsingular. Therefore, the matrix pencil (J_0, K_0) has no purely imaginary generalized eigenvalues. The equivalence of 1) and 2) also implies $M_0 > 0$, therefore, 3) can be derived from 2) and the above statements are equivalent. ■

We remark that GARE requires (E, A) to be impulse-free, but GHM does not. Furthermore, GHM can locate the passive/nonpassive regions whereas GARE can not.

V. Numerical Examples

This section presents some numerical examples to verify the proposed passivity test flow. All experiments are performed in MATLAB R2006a on a 2.66 GHz 2G-RAM PC.

TABLE I
GHM test results for the reduced model.

Imaginary generalized eigenvalues of (J_0, K_0)	$H_r(j\omega)$
3.65e-13 $\pm\ j3.3078$	0.0000 $+j0.0031$
5.00e-14 $\pm\ j1.2345$	0.0000 $-j0.0060$

An MNA Example for ImPT: This 9-port order-10913 model describes a large RLC network. Since the RLC circuit is passive, ζ should be 1 or 2 and $M_1 \geq 0$. To show the convergence of ImPT, we set $s_1 = 10^3$ and $\eta = 10$, and plot the numerical error ε_i for $i = 1, 2, .., 6$ in Fig. 3(a), which shows ε_i decreases by about 2 orders each iteration. Setting $s_i = 10^4$ and $s_{i+1} = 10^5$ in (19) yields $\zeta = 2$ after 2.1 seconds. The magnitude of port-2 to port-2 frequency response in Fig. 3(b) increases linearly in the high-frequency band, which also implies $\zeta = 2$. Via (20), we get a 9×9 diagonal matrix with positive diagonal elements, so $M_1 > 0$. To verify the numerical accuracy of M_1, we compute ζ of the "proper part" $H_1(s) = H(s) - sM_1$ by (19). We get $\zeta = 1$ for $H_1(s)$, implying $H_1(s)$ is impulse-free as expected. Meanwhile, the port-2 to port-2 response of $H_1(s)$ in Fig. 3(c) also shows $H_1(s)$ has no impulsive part. This example shows that ImPT is efficient and accurate in practical implementations.

A PEEC Example for GHM: The SISO order-51 reduced model is obtained by performing PRIMA [2] on a PEEC DS model of dimension 480 with $D = 0$. Both of them are nonpassive in the low-frequency band. ImPT shows they are impulse-free. After equivalent model conversion, GHM test on the original model produces 59 crossover points. We compute the transfer functions at these 59 points (denoted by $H_c(s)$). Fig. 4 shows that the real part of $H_c(s)$ is zero. By frequency sweeping, we get 29 boundary frequency points. The frequency sweeping result $H_s(s)$ is plotted in Fig. 4. We note that all these 29 points are also detected by GHM. However, the other 30 crossover points are missed in frequency sweeping test. Therefore, GHM is more reliable than frequency sweeping. For the reduced model, GHM produces 4 purely imaginary results listed in Table I, which represent 2 crossover frequency points. We also plot the real part of the transfer function of the reduced model ($H_r(s)$) in Fig. 5. The GHM results are accurately located at the crossover points of $real(H_r(s))$ with x-axis. We note that GHM test results in Table I contain some numerical noise in the real parts, which is also observed in traditional Hamiltonian method [5].

A SAW Filter for HGHM: This order-126 admittance symmetric DS is from a 3-terminal SAW filter. ImPT shows

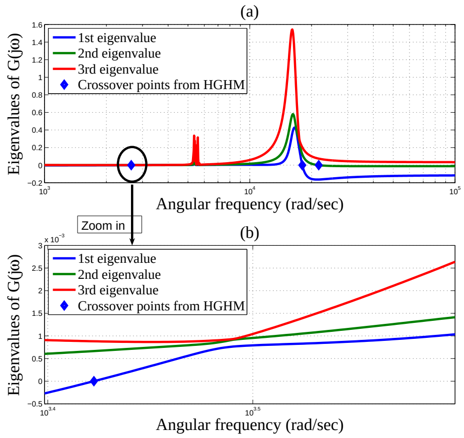

Fig. 6. HGHM test for the SAW model.

TABLE II
GHM AND HGHM TEST RESULTS FOR THE SAW MODEL.

Imaginary results of GHM	Positive results of HGHM (β)	$\sqrt{\beta}$
-1.4e-8 $\pm j21671.377$	469648579	21671.377
-1.9e-8 $\pm j18029.84$	325075192.6	18209.84
3.38e-8 $\pm j2645.316$	6997698.35	2645.316

this DS is impulse-free. HGHM test produces 3 positive real generalized eigenvalues, and GHM test produces 6 imaginary generalized eigenvalues. Table II shows that the results from GHM test have numerical noise in the real parts, but HGHM does not suffer from this problem. The 3 crossover frequency points from HGHM are plotted in Fig. 6, which shows the HGHM test is very accurate.

CPU Time Comparison: We compare the CPU timing of GHM and HGHM with two decompose-and-test methods: SHH [13] and Weierstrass passivity tests [14]. For fairness, in decompose-and-test routines the proper parts are tested by Hamiltonian method. Experiments are performed on some symmetric DSs with order from 50 to 800. The CPU times of GHM, HGHM, SHH and Weierstrass passivity tests are listed in Table III. It is shown that HGHM is about $8\times$ faster than GHM, which is expected due to its half-size property. GHM is ($> 2\times$) faster than SHH. The additional cost of SHH is mainly from system decompositions. GHM, HGHM and SHH are all faster than Weierstrass test, which coincides with the observations in [13].

VI. CONCLUSION

A new DS passivity test flow based on GHM/HGHM has been proposed for the first time. The most significant advantage of this method is its ability of accurately detecting the possible nonpassive regions, some of them may be missed with frequency sweepings. With ImPT and equivalent model conversion, GHM and HGHM are applicable to general and symmetric DSs, respectively, without system decompositions. Experiments have demonstrated the much higher accuracy of GHM than frequency sweeping, and faster computation than SHH and Weierstrass tests. In symmetric DSs, HGHM enjoys an $8\times$ speedup and a higher numerical accuracy over GHM.

TABLE III
CPU TIMES OF DIFFERENT DS PASSIVITY TESTS (sec).

Model order	Weierstrass	SHH	GHM	HGHM
50	0.2270	0.0781	0.0156	0.0013
100	0.4470	0.2969	0.1406	0.0156
150	1.1093	0.9375	0.3906	0.0625
200	2.6872	2.3281	0.8706	0.1250
300	10.725	8.2500	3.3750	0.3906
400	32.781	20.125	7.7938	0.8906
500	51.676	39.719	17.328	1.7788
600	124.83	69.208	25.813	2.9688
700	161.21	108.40	38.906	4.9219
800	289.37	166.64	65.670	7.6406

REFERENCES

[1] P. Feldmann and R. Freund, "Reduced-order modeling of large linear subcircuits via a block Lanczos algorithms," in *Proc. ACM/IEEE Design Autom. Conf.*, 1995, pp. 474–479.

[2] A. Odabasioglu, M. Celik, and L. Pileggi, "PRIMA: passive and reduced-order interconnect macromodeling algorithm," *IEEE Trans. Comput.-Aided Design*, vol. 17, no. 8, pp. 645–654, Aug 1998.

[3] S. Grivet-Talocia and A. Ubolli, "A comparative study of passivity enforcement schemes for linear lumped macomodels," *IEEE Trans. Advanced Packaging*, vol. 31, no. 4, pp. 673–683, Nov 2008.

[4] B. Gustavsen and A. Semlyen, "Rational approximation of frequency domain responses by vector fitting," *IEEE Trans. Power Delivery*, vol. 14, no. 3, pp. 1052–1061, July 1999.

[5] A. Semlyen and B. Gustavsen, "A half-size singularity test matrix for fast and reliable passivity assessment of rational models," *IEEE Trans. Power Delivery*, vol. 24, no. 1, pp. 345–351, Jan 2009.

[6] E. L. Yip and R. F. Sincovec, "Solvability, controllability and observability of continuous descriptor systems," *IEEE Trans. Automat. Control*, vol. AC-26, no. 3, pp. 702–707, 1981.

[7] L. Dai, *Singular Control Systems*, ser. Lecture Notes in Control and Information Sciences 118. Berlin/Heidelberg: Springer-Verlag, 1989.

[8] H. Heeb and A. Ruehli, "Three-dimensional interconnect analysis using partial element equivalent circuits," *IEEE Trans. Circuits Syst. I*, vol. 39, no. 11, pp. 974–982, Nov 1993.

[9] R. Freund, "An extension of positive real lemma to descriptor systems," *Optim. methods and software*, vol. 19, no. 1, pp. 69–87, Feb 2004.

[10] D. Chu and R. C. E. Tan, "Algebraic characterizations for positive realness of descriptor systems," *SIAM J. Matrix Anal. Appl.*, vol. 30, no. 1, pp. 197–222, 2008.

[11] C. Yang, Q. Zhang, Y. Lin, and L. Zhou, "Positive realness and absolute stability problem of descriptor systems," *IEEE Trans. Circuits Syst. I*, vol. 54, no. 5, pp. 1142–1149, May 2007.

[12] L. Zhang, J. Lam, and S. Xu, "On positive realness of descriptor systems," *IEEE Trans. Circuits Syst. I*, vol. 49, no. 3, pp. 401–407, Mar. 2002.

[13] N. Wong and C. Chu, "A fast passivity test for stable descriptor systems via skew-Hamiltonian/ Hamiltonian matrix pencil transformations," *IEEE Trans. Circuits and Syst. I*, vol. 55, no. 2, pp. 635–643, Mar 2008.

[14] P. Benner and D. Chu, "A new test for passivity of descriptor systems," Nov 2005, mathematisches Forschungsinstitut Oberwolfach.

[15] Z. Bai and R. Freund, "Eigenvalue-based characterization and test for positive realness of scalar transfer functions," *IEEE Trans. Autom. Contr.*, vol. 45, no. 12, pp. 2396–2402, Dec 2000.

[16] Y. Liu and N. Wong, "Fast sweeping methods for checking passivity of descriptor systems," in *Proc. IEEE Asia Pacific Conf. on Circuits Syst.*, Dec 2008, pp. 566–569.

[17] N. Wong, "An efficient passivity test for descriptor systems via canonical projector techniques," in *Proc. ACM/IEEE Design Autom. Conf.* San Fransisco, CA, Jul 2009, pp. 957–962.

[18] Z. Zhang, C. U. Lei, and N. Wong, "GHM: a generalized Hamiltonian method for passivity test of impedance/admittance descriptor systems," in *Proc. Intl. Conf. Computer-Aided Design* San Jose, CA, Nov 2009, pp. 767–773

[19] R. Ionutiu, J. Rommes, and A. Antoulas, "Passivity-preserving model reduction using dominant spectral-zero interpolation," *IEEE Trans. Comput.-Aided Design*, vol. 27, no. 12, pp. 2250–2263, Dec 2008.